Toughening Mechanisms in SiC–TiC Composites

SiC–TiC 複合材の高靱化機構

Young-Il LEE and Young-Wook KIM

Department of Materials Science and Engineering, The University of Seoul, 90 Jeonnong-Dong, Dongdaemoon-Ku, Seoul 130-743, Republic of Korea

Three different microstructures in SiC–TiC composites containing Al_2O_3 and Y_2O_3 as sintering additives were prepared by hot-pressing and subsequent annealing. To investigate the dominant toughening mechanism operating in toughened SiC–TiC composites, the microstructure-crack interaction was examined by image analysis. Crack deflection by elongated α-SiC grains was most frequently observed (61% of the observed sites) as the dominant toughening mechanism in the SiC–TiC composites. Crack deflection was generally observed for elongated α-SiC grains with aspect ratio (AR) > 2.5 and grain thickness (t) < 2.5 μm. Crack bridging (21% of the observed sites) was also observed as one of the operating toughening mechanisms. The rest (18%) of the observed grains fractured transgranularly. The crack bridging mechanism was mostly related to thinner grains with thickness $t < 2$ μm, while transgranularly fractured elongated-grains were mostly related to thicker grains with thickness $2 < t < 4$ μm.

1. Introduction

Several investigations on SiC–TiC composites have shown that anisotropically grown α-SiC grains (hereafter "elongated grains" in a two-dimensional image) promote an increment of toughness in the presence of a relatively weak interface.[1]–[4] A fracture toughness of ~6.2 MPa·m$^{1/2}$ has been reported in SiC–TiC nanocomposites with needlelike microstructure,[1],[2] and a higher fracture toughness of 6.9 MPa·m$^{1/2}$ was reported in toughened SiC–TiC composites with yttrium aluminum garnet (Y$_3$Al$_5$O$_{12}$, YAG) as a grain boundary phase.[4] Attempts to introduce elongated SiC grains into the microstructure involves one of the following two strategies: (i) taking advantage of the $\beta \rightarrow \alpha$ phase transformation of SiC at high temperatures, which usually accelerates grain growth of SiC in the presence of TiC,[4]–[6] or (ii) using the chemical vapor deposition (CVD) process.[1],[2] The latter efforts include the codeposition of SiC and TiC to fabricate SiC–TiC nanocomposites with needle-like microstructure.[1],[2] These elongated grains can act as a reinforcing phase that promotes crack bridging and deflection, resulting in improved fracture toughness. For this to occur, the elongated grains must remain intact as the crack front approaches and passes them. This can happen if it is easier for the crack front to deflect along a basal plane of the hexagonal platelet (α-SiC grains) rather than to cut through the grain. The occurrence of toughening mechanisms depends on the grain morphology (i.e., microstructural characteristics) and the toughness of the intergranular film, which is controlled by the chemistry of sintering additives.[7],[8]

Some recent publications focused on the relationship between the processing, microstructure, and toughness in SiC–TiC composites.[4]–[6] Crack deflection and crack bridging were suggested as operating mechanisms in toughened SiC–TiC composites.[4],[6],[9] The present paper experimentally examines the microstructure-crack interaction in the SiC–TiC composites with different microstructures, which were prepared by varying heat-treatment conditions and polytype composition of the starting powders, without changing the additive composition. Analysis is based on geometric features of SiC grains, i.e., the thickness (t), length (l), and aspect ratio (AR) of the SiC grains. Based on the analysis, the relationship between the geometric features of SiC grains and the toughening mechanism is discussed, and the dominant toughening mechanism operating in these SiC–TiC composites is suggested.

2. Experimental procedure

Commercially available β-SiC (Ultrafine, Ibiden Co., Ltd., Nagoya), α-SiC (A–1 grade, Showa Denko, Tokyo), TiC (grade C.A.S., H. C. Starck, Berlin, Germany), Al_2O_3 (99.9% pure, Sumitomo Chemical Co., Tokyo), and Y_2O_3 (99.9% pure, Shin-Etsu Chemical Co., Tokyo) were used as the starting powders. Two batches of powders were mixed, each containing 60 mass% SiC, 30 mass% TiC, 4.3 mass% Al_2O_3, and 5.7 mass% Y_2O_3. The individual batches were ball-milled separately in ethanol for 24 h using SiC grinding balls and a jar. The milled slurry was dried, sieved, and hot-pressed at 1820°C for 1 h under a pressure of 25 MPa in an argon atmosphere. The hot-pressed samples were heated further at 2000°C for 6 h or 12 h under an applied pressure of 25 MPa in an argon atmosphere to enhance grain growth. The heating rate was 20°C/min, and the cooling rate was ~70°C/min from the heat-treatment temperature to 1200°C. The batch compositions and sample designations are given in **Table 1**.

The relative densities of the annealed samples were determined by the Archimedes method using deionized water as an immersion medium. The theoretical density of the samples, 3.707 g/cm^3, was calculated according to the rule of mixtures. X-ray diffractometry (XRD), using Cu Kα radiation, was performed on the ground powders. The hot-pressed and annealed samples were cut and polished. Microstructure-crack interactions were investigated for cracks

Table 1. Batch Composition, Annealing Conditions, and Relative Density of Samples

Sample	Batch Composition / mass%	Annealing Condition (°C/h/MPa)	Relative Density / %	Fracture Toughness / MPa·m$^{1/2}$
1	59.4% β-SiC† + 0.6% α-SiC‡ + 30% TiC¶ + 4.3% Al_2O_3 + 5.7% Y_2O_3	2000/6/25	98.2	6.8 ± 0.2
2	59.4% β-SiC + 0.6% α-SiC + 30% TiC + 4.3% Al_2O_3 + 5.7% Y_2O_3	2000/12/25	97.1	6.2 ± 0.1
3	60% α-SiC + 30% TiC + 4.3% Al_2O_3 + 5.7% Y_2O_3	2000/6/25	97.4	6.5 ± 0.2

† Ultrafine, Ibiden Co., Ltd., Nagoya, Japan

‡ A-1 grade, Showa Denko, Tokyo, Japan

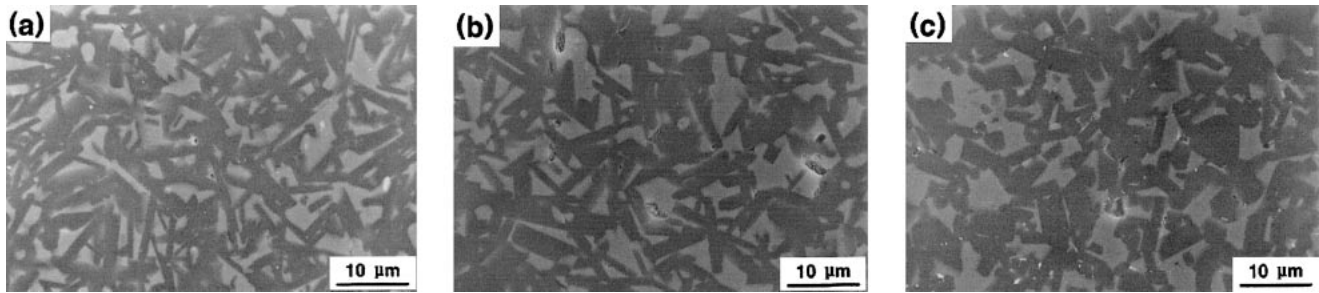¶ C. A. S. grade, H. C. Starck, Berlin, Germany

Fig. 1.   Microstructures of annealed SiC–TiC composites: (a) sample 1, (b) sample 2, and (c) sample 3 (refer to Table 1).
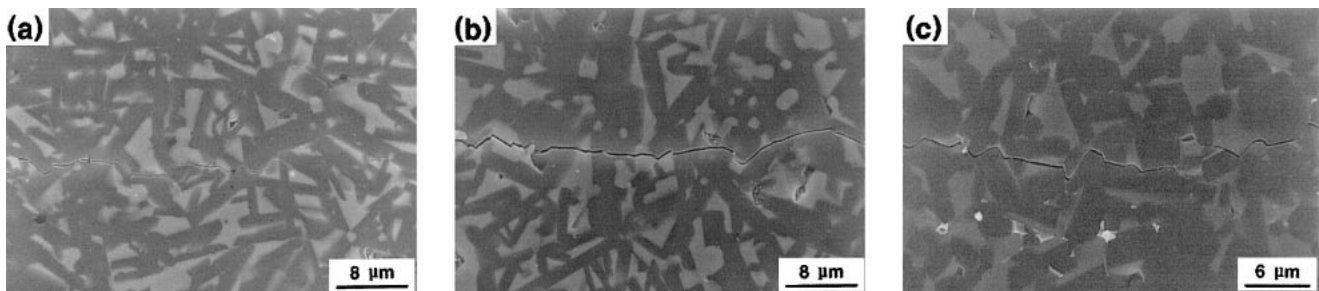

Fig. 2.   SEM micrographs of crack profiles in annealed samples: (a) sample 1, (b) sample 2, and (c) sample 3 (refer to Table 1).

introduced by a Vickers indenter at a load of 196 N on the polished surfaces. Then, the samples were etched by a plasma of CF_4 containing 7.8% O_2 for image analysis. The microstructures and the microstructure-crack interactions were observed by scanning electron microscopy (SEM). The grains interacting with a propagating crack were quantitatively analyzed by image analysis (Image-Pro Plus, Media Cybernetics, Maryland, U.S.A.), according to a procedure shown in a previous study.[8] Definitions of microstructural characteristics are demonstrated in Ref. 8. The thickness (t) of each grain was determined directly from the shortest grain dimension in its two-dimensional image; the apparent length (l) of each grain was obtained from the longest dimension. The mean value of the observed aspect ratio (l/t) was considered to be an average aspect ratio.

The fracture toughness was estimated by measuring the lengths of cracks that were generated by a Vickers indenter.[10] The variation of fracture toughness with indentation load (R-curve-like behavior) was estimated by changing the indentation load over a range of 49–294 N, and the toughness values that were measured in the steady-state region were reported in this study.

3.   Results and discussion

All samples showed relative densities of >97% after annealing under pressure (Table 1). The microstructures of the sintered and annealed samples are shown in **Fig. 1**. The bright phase is TiC and the dark phase is SiC. All samples showed microstructures similar to typical *in situ*-toughened ceramics, consisting of elongated α-SiC grains and matrix-like TiC grains. However, the morphology of SiC grains was different depending on the polytype of the starting SiC powders and the annealing conditions. Sample 1 (Fig. 1 (a)) prepared from β-SiC containing 1 mass% α-SiC shows more elongated grains whereas sample 3 (Fig. 1(c)) prepared from α-SiC shows less elongated grains. The difference in morphology of SiC grains reflects different growth behavior of SiC grains. The grain growth of SiC grains in sample 1 has resulted from an overgrowth of β-SiC on α-SiC seeds during hot-pressing, resulting in the formation of α/β composite grains.[11] Strain at the

α/β interface accelerated the elongation of the grains by the $\beta \rightarrow \alpha$ phase transformation of SiC during annealing,[12),13)] resulting in a higher aspect ratio of SiC grains than sample 3. Phase analysis of the annealed samples by XRD revealed α-SiC and TiC as major phases and $Y_3Al_5O_{12}$ as a trace, indicating the occurrence of $\beta \rightarrow \alpha$ phase transformation of SiC during annealing. It is well documented that the $\beta \rightarrow \alpha$ phase transformation of SiC led to the *in-situ* growth of elongated α-SiC grains.[4),14)] In contrast, the grain growth in sample 3 has resulted from the solution-reprecipitation mechanism, i.e., growing of larger relatively equiaxed α-SiC grains by consuming relatively small α-SiC grains, without the $\beta \rightarrow \alpha$ phase transformation of SiC.[15] When the annealing time was increased, the thickness of grains increased, but the aspect ratio decreased because of the impingement of growing grains (see Figs. 1(a) and (b)).

The crack paths, introduced by Vickers indentation, were investigated to analyze the toughening mechanisms. SEM observation on crack paths suggests the occurrence of both crack deflection and crack bridging by elongated SiC grains as operating toughening mechanisms in these composites (**Fig. 2**). Another possible mechanism is microcrack toughening, owing to the thermal expansion mismatch between the SiC and TiC grains. Kleebe[16] reported that the predominant toughening mechanism in SiC with YAG as a secondary phase was microcrack toughening. Hence, the contribution of microcrack toughening cannot be ruled out in these composites. However, it is largely accepted that crack bridging and deflection are the dominant toughening mechanisms in these composites.[3),4),9),17)] Transgranular fracture of some grains was also observed. The observed toughening mechanisms changed with respect to the morphology of SiC grains. The 6 h annealed samples (samples 1 and 3) showed tortuous crack paths and demonstrated significant crack bridging and deflection by elongated SiC grains, as shown in Figs. 2(a) and (c). In contrast, 12 h-annealed samples showed an increased tendency for the transgranular fracture. The fracture toughness of 6-h annealed sample (sample 1) was 6.8 MPa·m$^{1/2}$ (Table 1). Further annealing up to 12 h (sample 2) decreased the fracture toughness
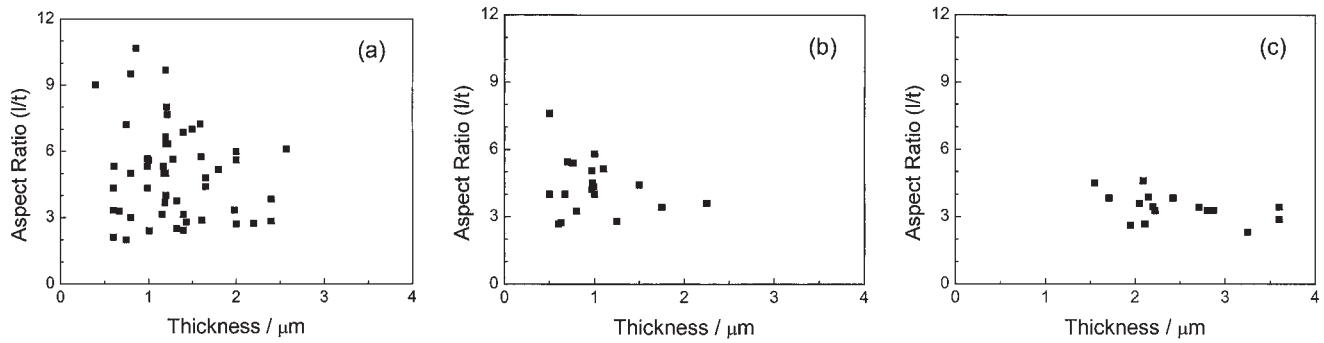
Fig. 3.   Relation between aspect ratio and thickness of SiC grains observed at (a) crack deflection sites, (b) crack bridging sites, and (c) cut-elongated-grains in SiC–30 mass% TiC composites.

(6.2 MPa·m$^{1/2}$) slightly, although the thickness and the length of α-SiC grains were increased. This could be attributed to the increasing tendency of the transgranular fracture with the prolonged annealing. It should be mentioned that the fracture toughness values are relative values (not absolute values), because they were measured by indentation method.[10]

All grains interacting with a propagating crack were quantitatively analyzed by image analysis. The grains interacting with a propagating crack were classified into three principal categories: (i) grains observed at crack deflection sites (designated as deflection grains); (ii) grains observed at crack bridging sites (bridging grains); and (iii) grains fractured transgranularly (cut elongated grains).

The aspect ratio-thickness relation of SiC grains observed at the microstructure-crack interaction sites are shown in **Fig. 3**. Crack deflection mechanism was mostly related to elongated α-SiC grains with $t < 2.5\,\mu$m and $AR > 2.5$ (Fig. 3(a)). The crack deflection was most frequently observed in the SiC–30 mass% TiC composites. Crack bridging was generally observed for elongated α-SiC grains with $t < 2\,\mu$m and $AR > 3$ (Fig. 3(b)). The grain was partially debonded along the relatively weak interface boundaries and acted in a definite time period as an elastic bridging for the propagating crack. Cut-elongated grains were related to α-SiC grains with $2\,\mu$m $< t < 4\,\mu$m and $2 < AR < 4.5$ (Fig. 3(c)). The average values of length, thickness and aspect ratio of SiC grains belonging to each category are compared in **Fig. 4**. Generally, grains contributing to crack bridging were thinner and shorter than the grains contributing to crack deflection. Cut elongated grains were thicker and longer than the grains contributing to the crack

deflection. The occurrence of the crack bridging mechanism was strictly limited to elongated grains with $t < 2\,\mu$m. This restriction can be explained as follows. At the moment when the crack tip is just behind the toughening grain, this grain is stressed by bending. Because thick grains are less flexible than thin ones, elongated SiC grains with $t > 2\,\mu$m may not act as bridges and fail during the period of bending, as observed in Fig. 2(b). Figure 4 also shows that grains with high aspect ratio are effective in creating crack deflection.

Among the SiC grains observed at the microstructure-crack interaction sites in all samples, 61% of the grains were related to crack deflection, 21% to crack bridging, and 18% to cut elongated grains. Present observation suggests that the dominant toughening mechanism operating in the present SiC–TiC composites is believed to be a crack deflection by elongated α-SiC grains. However, the dominant toughening mechanism may depend on the microstructure of the composites. In this study, there was no dramatic microstructural change between samples, although the annealing time and crystalline phase of the starting powders have been changed. This may be due to the impingement of growing SiC grains. The present results suggest that maximizing the volume content of SiC grains with $t < 2\,\mu$m and $AR > 3$, which are common grains for both crack bridging and deflection, is necessary for further improvement in toughness of the SiC–TiC composites.

4.   Conclusions

In situ-toughened SiC–TiC composites were prepared using SiC starting powders with different α:β phase ratios and different annealing conditions, using a constant Al$_2$O$_3$ and Y$_2$O$_3$ sintering additive content. The resulting microstructures differed in the morphology of the SiC grains formed. Observation of crack-microstructure interaction suggests that the dominant toughening mechanism operating in toughened SiC–TiC composites was crack deflection by elongated SiC grains. SiC grains with $t < 2.5\,\mu$m and $AR > 2.5$ contributed to the toughening mechanism effectively.

Fig. 4.   Relation between microstructural parameter and toughening mechanism in toughened SiC–30 mass% TiC composites.

References

1) Gourbilleau, F., Maupas, H., Hillel, R. and Chermamt, J., *Mater. Res. Bull.*, Vol. 29, pp. 673–680 (1994).
2) Chermant, H., Chermamt, J. L. and Hillel, R., *Mater. Res. Bull.*, Vol. 29, pp. 895–902 (1994).
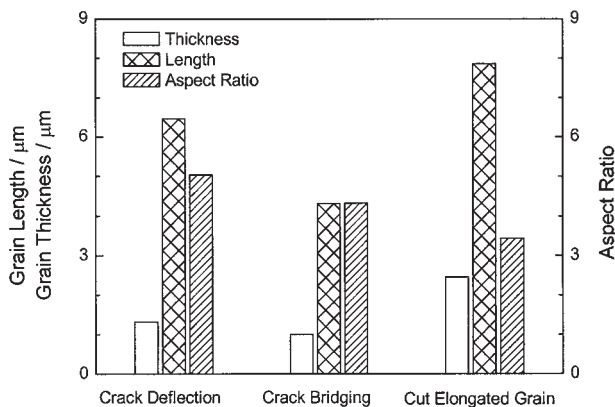3) Chae, K. W., Niihara, K. and Kim, D. Y., *J. Am. Ceram. Soc.*, Vol. 79, pp. 3305–3308 (1996).

4) Cho, K. S., Kim, Y.-W., Choi, H. J. and Lee, J. G., *J. Am. Ceram. Soc.*, Vol. 79, pp. 1711–1713 (1996).

5) Kim, Y.-W., Lee, S. G. and Lee, Y. I., *J. Mater. Sci.*, Vol. 35, pp. 5569–5574 (2000).

6) An, H. G., Kim, Y.-W. and Lee, J. G., *J. Eur. Ceram. Soc.*, Vol. 21, pp. 93–98 (2001).

7) Becher, P. F., Sun, E. Y., Hsueh, C. H., Alexander, K. B., Hwang, S. L., Waters, S. B. and Westmoreland, C. G., *Acta Mater.*, Vol. 44, pp. 3881–3893 (1996).

8) Lee, S. G., Kim, Y.-W. and Mitomo, M., *J. Am. Ceram. Soc.*, Vol. 84, pp. 1347–1353 (2001).

9) Kim, Y.-W. and Lee, Y. I., *Int. J. Mater. & Product Tech.*, Vol. 18, pp. 199–214 (2003).

10) Anstis, G. R., Chantikul, P., Lawn, B. R. and Marshall, D. B., *J. Am. Ceram. Soc.*, Vol. 64, pp. 533–538 (1981).

11) Kim, Y.-W., Mitomo, M. and Hirotsuru, H., *J. Am. Ceram. Soc.*, Vol. 80, pp. 99–105 (1997).

12) Ogbuji, L. U., Mitchell, T. E. and Heuer, A. H., *J. Am. Ceram. Soc.*, Vol. 64, pp. 91–99 (1981).

13) Ogbuji, L. U., Mitchell, T. E., Heuer, A. H. and Shinozaki, S., *J. Am. Ceram. Soc.*, Vol. 64, pp. 100–105 (1981).

14) Zhan, G. D., Mitomo, M., Tanaka, H. and Kim, Y.-W., *J. Am. Ceram. Soc.*, Vol. 83, pp. 1369–1374 (2000).

15) Kim, J. Y., Kim, Y.-W., Mitomo, M., Zhan, G. D. and Lee, J. G., *J. Am. Ceram. Soc.*, Vol. 82, pp. 441–444 (1999).

16) Kleebe, H. J., *J. Eur. Ceram. Soc.*, Vol. 75, pp. 151–159 (1992).

17) Cho, K. S., Choi, H. J., Lee, J. G. and Kim, Y.-W., *J. Mater. Sci. Lett.*, Vol. 17, pp. 1081–1084 (1998).